Infrared - X-ray pump probe spectroscopy

Viviane Costa Felicíssimo

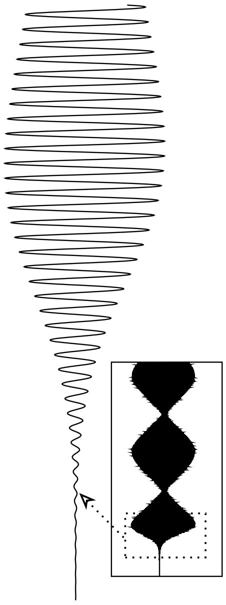

Theoretical Chemistry
Royal Institute of Technology
Stockholm, 2005

© Viviane Costa Felicíssimo, 2005
ISBN 91-7283-939-2
Printed by Universitetsservice US AB, Stockholm, 2005

Abstract

The present thesis concerns theoretical studies of molecular interactions investigated by infrared and X-ray spectroscopic techniques, with emphasis on using the two technologies combined in pump probe experiments. Three main types of studies are addressed: the use of near-edge X-ray absorption fine structure spectra (NEXAFS) to manifest through-bond and through-space interactions; the role of hydrogen bonding on the formation of X-ray photoelectron spectra as evidenced by simulations of the water dimer; and the development of theory, with sample applications, for infrared X-ray pump probe spectroscopy - the main theme of the thesis.

Ab initio calculations indicate that NEXAFS spectra give direct information about the through-bond and through-space interactions between vacant non-conjugated π^* orbitals. It is found that the X-ray photoelectron spectrum of the water dimer differs strongly from the monomer spectrum in that two bands are observed, separated by the chemically shifted ionization potentials of the donor and the acceptor. The hydrogen bond is responsible for the anomalously strong broadening of these two bands. The studies show that X-ray core electron ionization of the water dimer driven by an infrared field is a proper technique to prove the proton transfered state contrary to conventional X-ray photoelectron spectroscopy. Our simulations of infrared X-ray pump-probe spectra were carried out using wave packet propagation techniques.

The physical aspects of the proposed new X-ray spectroscopic method - phase sensitive Infrared - X-ray pump probe spectroscopy - are examined in detail in two sample applications - on the NO molecule and on the dynamics of proton transfer in core ionized water dimer. It is found that the phase of the infrared pump field strongly influences the trajectory of the nuclear wave packet on the ground state potential. This results in a phase dependence of the X-ray pump probe spectra. A proper choice of the delay time of the X-ray pulse allows to directly observe the X-ray transition in the proton transfered well of the core excited potential.

Preface

The work in this thesis has been carried out at the Laboratory of Theoretical Chemistry, Department of Biotechnology, Royal Institute of Technology, Stockholm.

List of papers included in the thesis

Paper I V.C. Felicíssimo, A. Cesar, Y. Luo, F. Gel'mukhanov, and H. Ågren, *Probing through-bond and through-space interactions by means of near-edge X-ray absorption spectroscopy. A theoretical study on non-conjugated diene molecules*, J. Phys. Chem. A (submitted) 2004.

Paper II V.C. Felicíssimo, I. Minkov, F.F. Guimarães, F. Gel'mukhanov, A. Cesar, and H. Ågren, *A theoretical study of the role of the hydrogen bond on core ionization of the water dimer*, Chem. Phys. (accepted) 2004.

Paper III V.C. Felicíssimo, F.F. Guimarães, F. Gel'mukhanov, A. Cesar, and H. Ågren, *The principles of IR - X-ray pump-probe spectroscopy. Applications on proton transfer in core ionized water dimer.*, J. Chem. Phys. (submitted) 2004.

Paper IV F.F. Guimarães, V. Kimberg, V.C. Felicíssimo, F. Gel'mukhanov, A. Cesar, and H. Ågren, *IR - X-ray pump-probe spectroscopy of the NO molecule*, Phys. Rev. A (submitted) 2004.

List of papers not included in the thesis

Paper I F.F. Guimarães, V. Kimberg, V.C. Felicíssimo, F. Gel'mukhanov, A. Cesar, and H. Ågren, *Phase sensitive X-ray absorption driven by strong infrared fields*, Phys. Rev. Lett. (submitted) 2004.

Acknowledgments

I would like to express my sincere thanks to my supervisor Faris Gel'mukhanov, a fascinating person, who provided me with a friendly atmosphere during the execution and preparation of this thesis. Thanks for the valuable knowledge I acquired with you.

I will be forever grateful to my Brazilian supervisor, Amary Cesar, for his constant encouragement and belief in me, and, mainly, for everything I have learned from him.

I am very thankful to Prof. Hans Ågren for inviting me to take part in his research group and for putting excellent work conditions at my disposal. I learned a lot during discussions with Hans and during his seminars.

My true thanks to Freddy for all working collaboration and friendship.

I am immensely grateful to Óscar for his companionship and friendship.

I would like to thank Luo, Ivo and Viktor who I had the pleasure to collaborate with.

Special thanks to Fahmi who during his “Friday's pub” explained the importance of the transition state in our daily life.

I also want to thank Barbara, Jing-Dong, Cornel and Elias for their pleasant company and discussions.

Thanks to Teresa and Matteo for good moments in Stockholm.

Thanks to the members of Theoretical Chemistry Group; Lotta, Boris, Pawel, Olav, Luca, Kathrin, Linnea, Polina, Zilvinas, Su, Jun Jiang, Mathias, Laban, Sergey, Lyudmyla, Yan-Hua, Liu, Emanuel, Peter, Yaoquan and Guangde for providing me a very harmonious working environment.

Thanks to everyone who directly or indirectly contributed for the development of this work.

I am very thankful to Katia and Márcia for their strength and friendship.

My deep gratitude to my unforgettable Brazilian friends for their constant affection.

I am eternally grateful to Jader for his essential strength and love.

To my dear family for its incessant optimism and love, thank you very much.

Thanks to CAPES - Coordenação de Aperfeiçoamento de Pessoal de Nível Superior (Brazil) for the 'sandwich' doctoral scholarship.

Contents

1 Introduction 9

2 NEXAFS and XPS studies of molecular interaction 13

- 2.1 Principle of NEXAFS 13
- 2.2 Principles of X-ray photoelectron spectroscopy (XPS) 14
- 2.3 Vibrational structure in X-ray spectra 16
- 2.4 Study of TB and TS interactions using NEXAFS 17
  - 2.4.1 Through-space interaction in ethylene dimer 17
  - 2.4.2 Through-bond interaction in the *p*-benzoquinone molecule 18
- 2.5 XPS study of hydrogen bonding in the water dimer 20

3 X-ray pump-probe spectroscopy 25

- 3.1 Principle of IR spectroscopy 26
- 3.2 Proton transfer in core ionized state of water dimer 27
- 3.3 Role of light coherence, duration and phase 31
  - 3.3.1 X-ray spectrum in the field of incoherent pump radiation 31
  - 3.3.2 Role of duration of X-ray and IR pulses 32
  - 3.3.3 Phase memory versus shape of the IR pulse 33
  - 3.3.4 Dephasing caused by z-dependence of the phase of the IR field 33

4 Conclusion 37

Chapter 1

Introduction

Molecular interactions are subject to great interest in chemistry, physics and biology because they are the keys to understand properties and structure of matter. Every substance is made up of atoms, and all atoms are surrounded by electrons. Essential to understanding of all types of chemical bonding is the realization that bonds use electrons as the "glue". By large, the difference between materials as diverse as diamond and graphite can be traced to how they are kept together by electrons forming chemical bonds.

The understanding and prediction of the properties of matter at the atomic level represents one of the great achievements of twentieth-century science. The outstanding development of quantum mechanical ideas and computational facilities have widened old roads and drastically changed the understanding of molecular interactions. In the last decades, studies of molecular interactions have shown a fascinating progress. This is a result not only of the development of new theoretical methods and complex computations, but, of course, because many new experimental technologies have become available for such studies. These advancements have made it possible to study molecular systems in gas phase, in liquids and in solids.

Spectroscopy serves as the main tool to probe molecular structure and intra/inter-molecular interactions. Perturbations resulting from molecular interactions affect spectra in various ways. Changes in the energy levels lead to shifts in absorption and emission peaks, appearance of new resonances, etc. Changes of the molecular wave functions results in the redistribution of intensities. The great challenge in any spectroscopic field is to find solutions of the inverse problem - to extract information about molecular interactions from spectral changes. The various spectroscopies permit in that context different aspects of the interactions to be studied.

In this thesis two different types of molecular interactions are studied. One is the intramolecular interaction of orbitals localized on different functional groups or chromophores of organic compounds. The study of this orbital interaction is of great interest in chemistry as well in biology because it is responsible, for example, for the role of electron-transfer. The concept of the building block is of general importance in the study of orbital interactions and spectroscopy. Indeed, one can often treat different functional groups as building blocks of a molecule. Such a concept is found to be extremely powerful in infrared (IR) spectroscopy as well as in X-ray spectroscopies which see clearly the fingerprints of different functional groups. The deviation of the molecular spectra from the spectra of individual functional groups gives information about the interaction between these groups. Localized orbitals can interact with each other directly through orbital overlap (through-space (TS) interaction) or indirectly, through other bonds in the molecule (through-bond (TB) interaction). The TB interaction may operate over long distances. The existence and distinction between through-bond and through-space interactions in non-conjugated unsaturated molecular systems were originally introduced by Hoffmann and co-workers in Refs.[1,2] These milestone articles triggered detailed investigations of TS and TB interactions by different spectroscopic techniques and stimulated also our study.

The second kind of molecular interaction which is studied in this thesis is the hydrogen bonding. Hydrogen bonds are formed by linking a hydrogen atom between two electronegative atoms. The hydrogen bond can occur as intramolecular as well as intermolecular. The intermolecular hydrogen bonds that hold together water molecules have a strength in between the weak van der Waals and the strong covalent bond. The hydrogen bond which determines the properties of water and ice is also very important in proteins and nucleic acids and therefore in life processes. We study in this thesis the hydrogen bonding in the core electron ionized water dimmer. Different experimental techniques are found to be useful in studies of these interactions: electron energy loss (EELS), electron transmission (ETS), ultraviolet (UV), electron moment (EMS), infrared (IR) and infrared pump probe spectroscopies. In this thesis we investigate theoretically the manifestation of these interactions in three qualitatively different spectroscopies, namely, near edge X-ray absorption fine structure (NEXAFS), X-ray photoelectron spectroscopy (XPS) and IR - X-ray pump probe spectroscopy, the latter being the main theme of the thesis.

X-ray spectroscopies have experienced a great progress in recent years due to the impact provided by the new generation of synchrotron radiation sources. Synchrotrons produce very intense, tunable and polarized electromagnetic radiation covering a wide range of the electromagnetic spectrum: X-ray, UV, IR, and visible light to which the human eye is sensitive. Soon the X-ray free electron lasers will be in operation, something that will drastically increase the brilliance of the produced light. The free electron laser will also provide the opportunity to study dynamical processes down to 100 fs of resolution. A way to study ultrafast processes on time scales down 0.1 fs is based on harmonic generation X-ray lasers.[3] Other ways to obtain short X-ray pulses are based on slicing techniques[4–6] ($\sim$ 50 fs) and on so-called wakefield-induced energy chirps[7] ($\sim$ 10 fs). A main theme of the thesis is that these large achievements in creation of new sources for ultrashort X-ray pulses will, when synchronized with short IR pulses, make IR - X-ray pump probe spectroscopy a most interesting topic for forthcoming experimental studies. The development of theory of X-ray pump probe spectroscopy and investigations of the physics of X-ray interaction with laser driven molecules yield the way to select more important applications of this new type of X-ray spectroscopy and to focus experimental research along promising directions. The development and applications of an IR X-ray pump probe theory is precisely the main effort conducted in this thesis.

The wave packet technique is a central theoretical tool used in the presented papers. This technique allows to study the dynamical aspects of molecular interactions. Due to the computational complexity of the 1D and 2D wave packet simulations we used parallel computers.

The thesis firstly presents a study of NEXAFS spectra of non-conjugated diene molecules possessing through-bond and/or through-space interactions. The effects caused by the hydrogen bonding in the formation of core-level XPS spectra of the water dimer is then analyzed. IR - X-ray pump probe spectroscopy is employed to study the dynamics of proton transfer in the core ionized water dimer. The different physical aspects of the proposed new type of X-ray spectroscopy - phase sensitive X-ray pump-probe spectroscopy - are studied in detail for the NO molecule.

Chapter 2

NEXAFS and XPS studies of molecular interaction

X-ray spectroscopy can be subdivided in a few branches: X-ray absorption,[8–10] X-ray emission,[9] resonant X-ray Raman scattering,[11–17] Auger,[18] and X-ray photoelectron spectroscopies.[9,19] Here we will focus our attention to X-ray absorption and core level XPS spectra.

2.1 Principle of NEXAFS

When X-rays path through a sample the intensity of the incident beam is reduced due to photoabsorption. The X-ray photons excite core electrons to an unoccupied molecular orbital when the photon energy is smaller than the core ionization potential (Fig.2.1). Near the photoionization threshold one can also observe weak transitions to so-called Rydberg levels. When the photon energy exceeds the ionization threshold, the core electron is excited to continuum states. These states differ qualitatively going from atoms to molecules. Due to the multiple scattering of the photoelectron on the surrounding atoms in a molecule, resonances then appear also in the continuum.[20,21] Such resonances are known as shape resonances. The alternative interpretation of the shape resonances is related to the effective barrier[22] which creates the quasi-stationary state (see Fig.2.1), the barrier is shaped by the molecular potential. Quite often the X-ray absorption profile is disturbed by weak two-electron transitions. Both near edge (NEXAFS) and extended X-ray absorption fine structure (EXAFS) spectroscopies are widely used in material sciences to study structure of compounds. We will restrict our attention in this thesis to NEXAFS spectra as shown schematically in Fig.2.1. As NEXAFS spectra are formed by transitions of core electrons of specific atoms to vacant orbitals which are very sensitive to inter- and intra-molecular interactions, NEXAFS has become one of the most powerful tools in studies of molecular interactions as well as molecular structure.

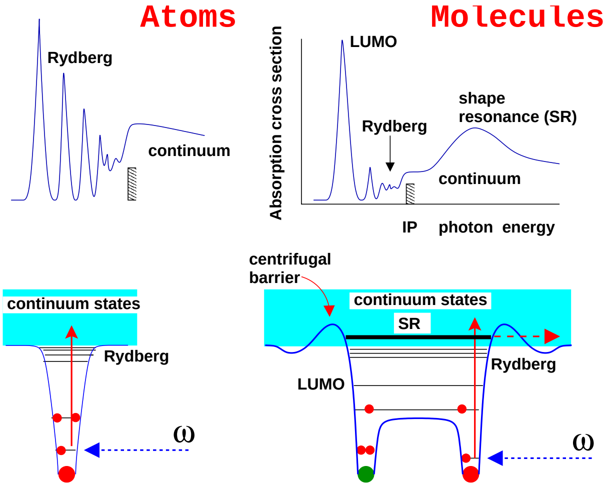
Atoms
Molecules
Rydberg
continuum
Absorption cross section
LUMO
Rydberg
shape resonance (SR)
continuum
IP
photon energy
centrifugal barrier
continuum states
Rydberg
ω
continuum states
SR
Rydberg
LUMO
ω

Figure 2.1: Formation of X-ray absorption spectra in atoms (left) and molecules (right).

2.2 Principles of X-ray photoelectron spectroscopy (XPS)

When the energy ω of the incident photon exceeds the ionization threshold, the molecule is ionized. The photoelectron spectrometer detects the emitted electron with certain energy and in certain direction. The change of the angle between the polarization vector $\mathbf{e}$ and the photoelectron momentum $\mathbf{k}$ allows to study the anisotropy of photoionization. Photoelectron spectroscopy gives direct information about occupied molecular levels. If the incident photon has high energy (X-ray photons), the photoelectron spectroscopy is designated as X-ray photoelectron spectroscopy (XPS). XPS maps both valence shells as well as core levels (Fig.2.2).

When the electron spectrometer detects photoelectrons with the binding energy

$$\mathrm{BE} = \omega - E \tag{2.1}$$

near the core ionization potential I_c one talks about core level XPS or ESCA (electron spectroscopy for chemical analysis). The XPS spectrum has resonances when

$$\mathrm{BE} = I_c. \tag{2.2}$$

In molecules, the ionization potential of the core electron experiences chemical shifts which are different for different atoms or atoms of the same chemical element but which are nonequivalent chemically. This has made XPS a powerful technique to study structure of molecules. This is illustrated in Fig.2.3 where we see that the O1s spectrum of the water dimer has two resonances. The origin of such a splitting is the nonequivalence of the two oxygen atoms in each water molecule which constitute the dimer. Thus, one oxygen has the donor role (O_d) and the other oxygen is an acceptor (O_a).

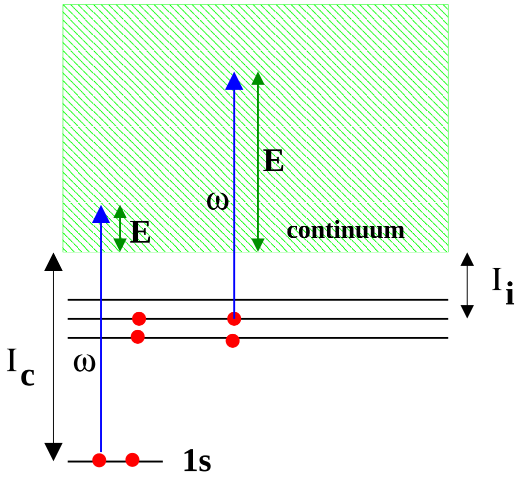

Figure 2.2: Principle of XPS or ESCA spectroscopies.

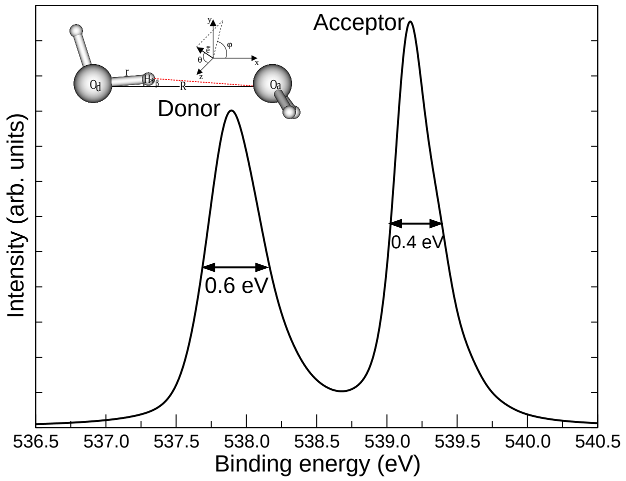

Figure 2.3: X-ray photoelectron spectrum of water dimer splitted due to different chemical shifts of donor and acceptor oxygens.

2.3 Vibrational structure in X-ray spectra

X-ray absorption as well as core ionization transitions in molecules also show fine structure caused by vibrations[8,19,23] (see Fig.2.4). The origin of such vibrational structure is the change of the shape and position of the potential surface of the core excited state relative to the ground electronic state. Quite often the potential of the core excited state is dissociative. In this case the X-ray resonance experiences dissociative broadening. The shape of a vibrational profile is defined by the overlap between vibrational wave functions of initial and final states or Franck-Condon (FC) amplitudes. In the harmonic approximation this amplitude results in a Poisson distribution[23,24]

$$\prod_{\alpha}\langle 0_\alpha|\nu_\alpha\rangle, \quad \langle 0_\alpha|\nu_\alpha\rangle \approx \frac{S_\alpha^{\nu_\alpha/2}}{\sqrt{\nu_\alpha!}}\, e^{-S_\alpha/2}, \quad S_\alpha = \frac{F_\alpha^2}{2\omega_\alpha^3} \tag{2.3}$$

where S_α is the partial Huang-Rhys (HR) parameter of the $\alpha\ th$ vibrational mode with the frequency ω_α. $F_\alpha = \partial E_c/\partial Q_\alpha$ is the gradient of the energy of the core excited state in the point of the vertical transition. The gradient, F_α, is the main parameter which defines the FC distributions for both bound-bound and bound-continuum transitions (see Fig.2.4).

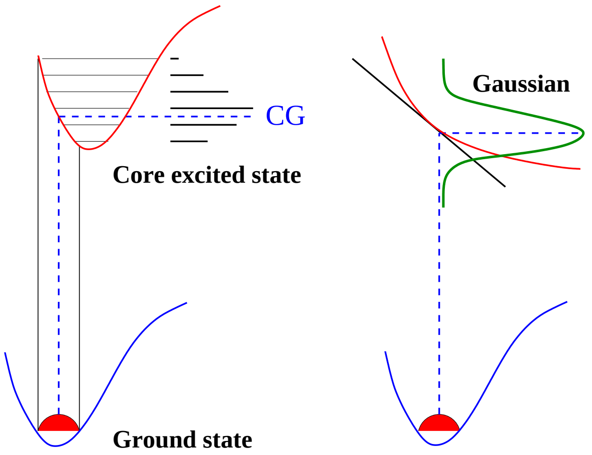

Figure 2.4: Vibrational broadening of NEXAFS and XPS spectra. Left and right panels display schematically transitions to bound and dissociative core excited states, respectively.

2.4 Study of TB and TS interactions using NEXAFS

As was mentioned in the Introduction, two functional groups can interact through-space (TS) and/or through-bond (TB).[1,2] We decided to study if and how NEXAFS spectroscopy can manifest such interactions of unoccupied orbitals. Below we highlight two illuminating results of these studies.

2.4.1 Through-space interaction in ethylene dimer

Let us start from the simplest case of NEXAFS spectra of the ethylene dimer (Fig.2.5).

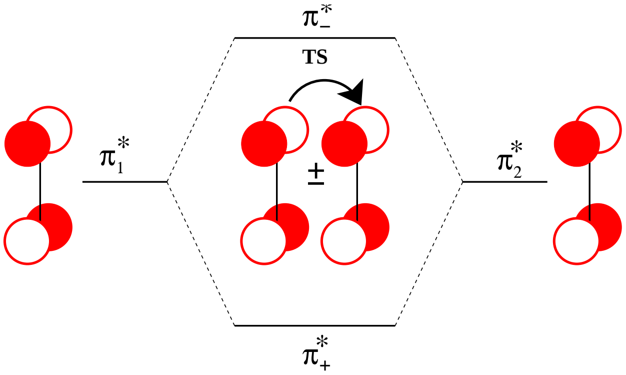

Figure 2.5: Illustration of the TS interaction in the ethylene dimer.

Two ethylenic groups do not interact when they are separated (R=∞). In this case the $C_2H_4 \cdots C_2H_4$ system has two degenerate unoccupied orbitals, π_1^* and π_2^*, which means that the NEXAFS spectrum displays a single strong resonance (see Fig.2.6) caused by the transition

$$1s \to \pi_{1,2}^* \tag{2.4}$$

in isolated ethylene. The NEXAFS spectrum of the ethylene dimer at the distance R=5.3 Å does not show any difference from the spectrum corresponding to R=∞ because the interaction between the ethylene molecules is then still rather small. When the ethylenic groups approach each other they start to interact because of the increase of the overlap of the π^* orbitals (Fig.2.5). Such a TS interaction results in the splitting

$$\Delta\epsilon = \epsilon(\pi_-^*) - \epsilon(\pi_+^*) \propto \langle \pi_1^* | \pi_2^* \rangle, \quad \pi_{1,2}^* \to \pi_\pm^* = \pi_1^* \pm \pi_2^* \tag{2.5}$$

which thus is absent for large intermolecular distances. When the distance is small (R=2.5 Å), the two groups interact and form the dimer. In this case the splitting is large and is clearly resolved in the NEXAFS spectrum (Fig.2.6). This splitting evidences directly the TS interaction in the ethylene dimer. According to eq.(2.5) one can expect to see two peaks ($1s \rightarrow \pi^*_-$ and $1s \rightarrow \pi^*_+$) with the same intensities in the NEXAFS spectrum. However, the simulations show that the first peak has larger intensity (see Fig.2.6). The reason for this is that eq.(2.5) ignores the interaction of the $\pi^*_\pm$ electron with the core hole. As is well established this interaction quite often results in a strong enhancement of the first peak due to the so-called excitonic effect.[25]

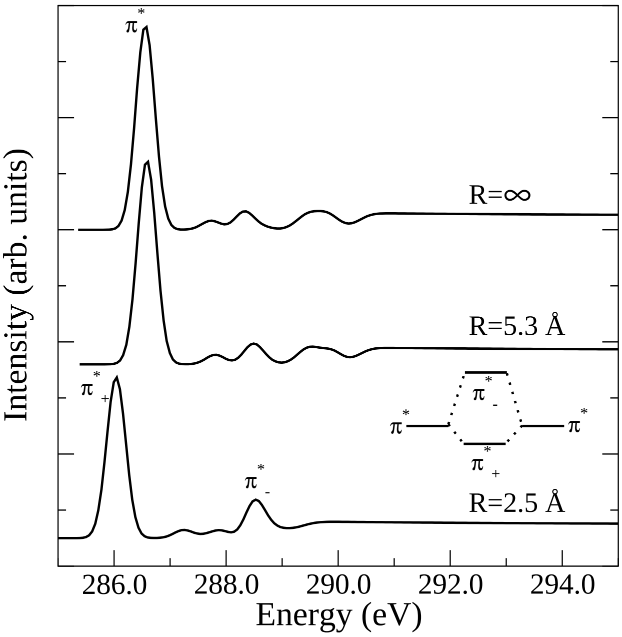

Figure 2.6: Theoretical C1s NEXAFS spectra of ethylene dimer at different R[($C_2H_4 \cdots C_2H_4$)] intermolecular distances (see Paper I).

2.4.2 Through-bond interaction in the *p*-benzoquinone molecule

Let us consider a qualitatively different mechanism of interaction between molecular orbitals localized on different functional groups. To be specific we consider the *p*-benzoquinone (pBQ) molecule. When two subsets (HC=CH)$\cdots$(HC=CH) and O=C$\cdots$C=O approach each other they interact and form the pBQ molecule. This interaction is depicted schematically in Fig.2.7. As it was shown in the previous subsection, the two ethylenic or carbonylic groups interact through the space. The rather weak TS interaction removes slightly the degeneracy of the π^*_+(C=C) and π^*_-(C=C) as well as of the π^*_+(C=O) and π^*_-(C=O) orbitals. A stronger interaction takes place between the effectively overlapping π^*_+(C=C) and π^*_-(C=O)

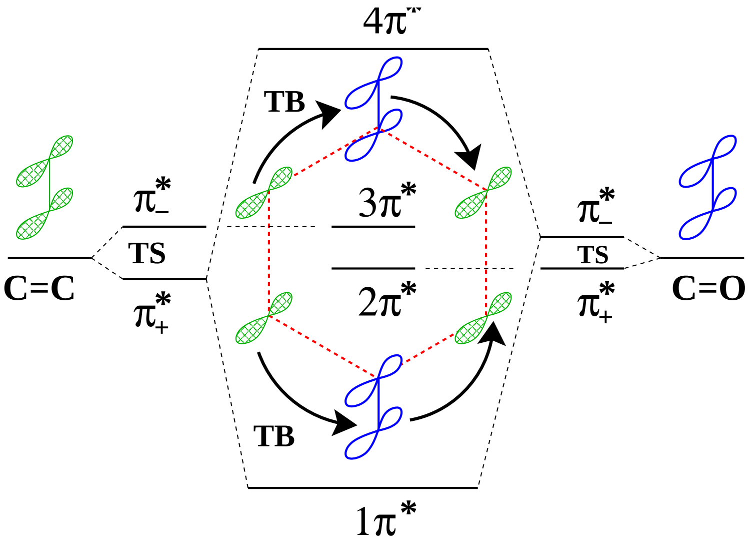

Figure 2.7: Illustration of the TB interaction in the pBQ molecule.

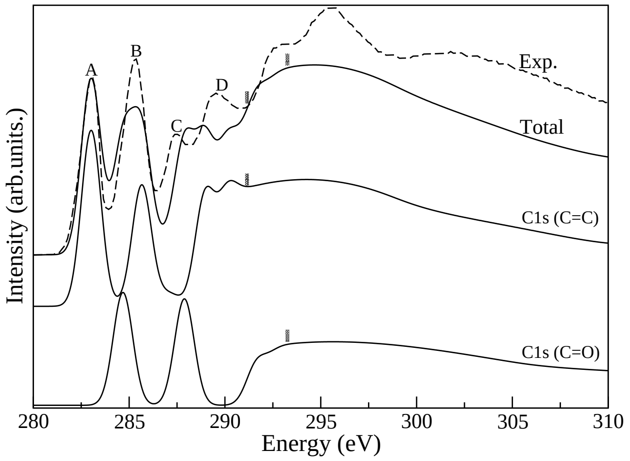

Figure 2.8: C1s NEXAFS spectrum of *p*-benzoquinone (pBQ) calculated by the DFT method. The experimental spectrum,[27] in broken lines, has been uniformly shifted so that the experimental and theoretical first π^* peak energies coincide.

orbitals which have appropriate symmetry to interact.[26] These orbitals form two new π^* molecular orbitals, $1\pi^*$ and $4\pi^*$, delocalized on the ethylenic and carbonylic groups. As it is illustrated in Fig.2.7 the π^* orbitals of the ethylenic groups interact indirectly, namely, they influence each other through the π^* orbitals of the carbonylic groups. This through-bond interaction is very strong and leads to a large splitting between the $1\pi^*$ and $4\pi^*$ orbitals. Our simulations (see Paper I) show that the interaction through-bond in pBQ is much stronger than through-space. The large TB splitting between the $1\pi^*$ and $4\pi^*$ orbitals is clearly seen in the partial C1s(C=C) NEXAFS spectrum, where the first and third peaks correspond to the transitions C1s(C=C) $\rightarrow 1\pi^*$ and C1s(C=C) $\rightarrow 4\pi^*$ (Fig.2.8). The A and D peaks in the total NEXAFS spectrum (Fig.2.8) correspond to transitions to the $1\pi^*$ and $4\pi^*$ orbitals, respectively. Thus these two peaks directly evidence the TB interaction in the pBQ molecule. The calculated spacing between the $1\pi^*$ and $4\pi^*$ transitions, 7.3 eV, is in good agreement with the experimental splitting[27] of 6.96 eV (Fig.2.8).

2.5 XPS study of hydrogen bonding in the water dimer

We shall now discuss another type of molecular interaction, namely, the hydrogen bond and its role in formation of XPS spectra of water dimer.

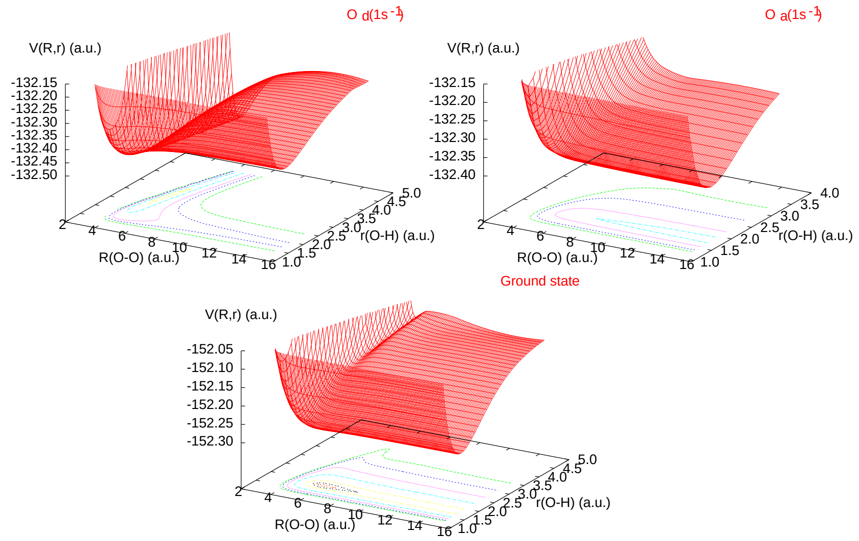

Figure 2.9: Potential surfaces of the ground state and core ionized states in donor and acceptor oxygens of water dimer.

The two water molecules in the ground state of the water dimer are weakly bound by the hydrogen bond.[28] The core ionization of the donor or acceptor oxygens of the water dimer results in a drastic change of the potential (see in Fig.2.9). The interaction between the two water molecules in the core-ionized state looks roughly like an ion-dipole interaction, which is much stronger than the dipole-dipole interaction between neutral polar molecules in the ground state. Contrary to the ground state, the global minimum is shifted to the proton transfer region when the core hole is created in the donor oxygen. In other words, the core ionization in the donor oxygen of the water dimer leads to a formation of a proton transfered state and consequently to a strengthening of the hydrogen bond.

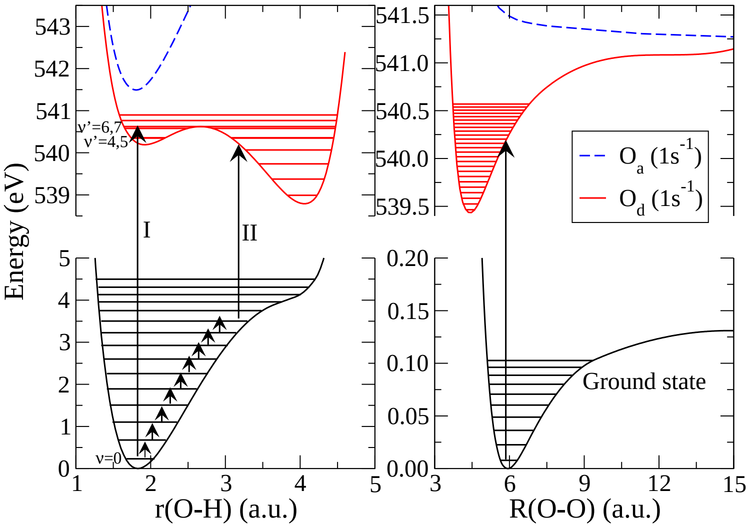

Figure 2.10: Potential surfaces of the ground state and core ionized states in donor and acceptor oxygens of the water dimer.

One can expect that asymmetry of the water dimer as well as change of the interaction between the monomers under core ionization strongly influence the XPS spectrum of the water dimer. Indeed, our simulations (Fig.2.3) show a qualitative distinction between XPS spectra of the dimer and the monomer[29] (see Fig.2.3 and Paper II). The photoelectron spectrum of the water dimer shows two very broad bands separated by 1.29 eV. This energy corresponds to the difference between the donor and acceptor O1s ionization potentials which have a characteristic shift to lower or higher energy, respectively. The vibrational fine structure observed in the monomer spectrum[29] is not resolved in the XPS spectrum of the water dimer due to the extra broadening caused by the drastic change of the core ionized potential in the region near the vertical transition along the low frequency intermolecular vibrational motions related mainly to the hydrogen bond. The origin of such a broadening is clearly seen from the right panel of Fig.2.10. This anomalous broadening is different for the donor (≈0.6 eV) and acceptor (≈0.4 eV) peaks. It is important to note that these different vibrational broadenings are due to weak hydrogen bonding which changes differently under core ionization of donor and acceptor oxygens (see right panel in Fig.2.10).

One can conclude that the broadenings and splitting in two vibrationally unresolved bands in the XPS spectrum of the water dimer serve as the fingerprints of the hydrogen bonding in the dimer. Unfortunately, the conventional XPS spectrum of the water dimer (Fig.2.3) does not reveal anything about the dynamics of proton transfer in the donor core ionized state. The reason for this is twofold; firstly, the proton transfer region is shifted too far away from the point of the vertical transition; secondly, the dynamics of the nuclear wave packet in the core-ionized state is rather slow compared with the lifetime of the core-ionized state (≈8 fs), see Fig.2.11.

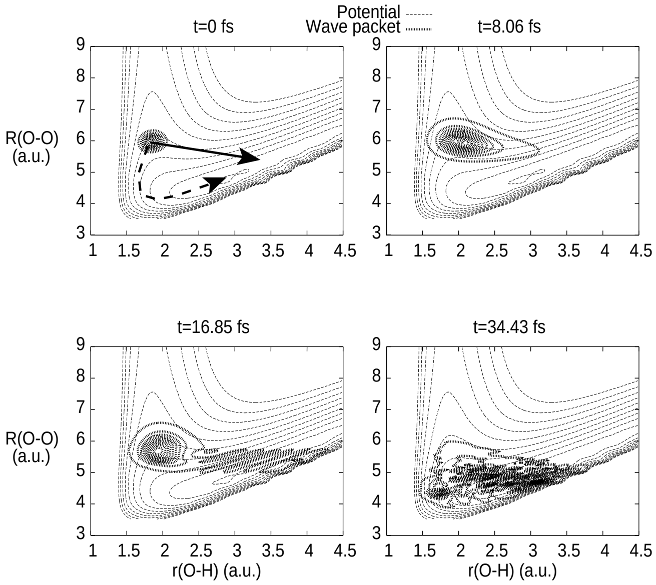

Figure 2.11: Propagation of the wave packet in donor core ionized potential surface. Continuous arrow shows over-barrier or tunneling path. The classical pathway is shown by dashed arrow.

The wave packet can reach the proton transfer region in the donor core ionized potential by two pathways: tunneling (or over-barrier) propagation and along the classical trajectory. The classical pathway starts from a slow approach of the heavy monomers followed by a quick transfer of the light proton along the r(O-H) coordinate. Our simulations show that the propagation of the wave packet along the classical pathway is indeed very slow. The bottleneck here is the slow motion along O-O which takes $\approx$ 28-34 fs (Fig.2.11). However, the dynamics of proton transfer by the way of tunneling or over-barrier motion takes smaller time, $\approx 8 - 16$ fs, which actually is comparable with the lifetime of the core ionized state. As one can see from Fig.2.11, a part of the wave packet has time to approach the proton transfer region during 8 fs. The appearance of the wave packet in the proton transfer region can be detected making use of Auger or X-ray emission spectroscopies.

Chapter 3

X-ray pump-probe spectroscopy

We have shown in the previous section that conventional XPS spectroscopy is not able to register the spectral transitions to the proton transfer region. However, it is possible to accomplish this by exciting the OH stretching mode using an IR pulse and measuring the XPS spectrum of such a vibrationally excited molecule (see Fig.3.1). Let us first describe the principle of IR - X-ray pump probe spectroscopy. Some applications of this technique is presented in Sec.3.2 for the study of proton transfer in the core ionized water dimer. In section 3.3 the benefits of X-ray pump probe spectroscopy are explored for the NO molecule.

It is worthwhile to note that the time independent and time resolved pump probe schemes have served as revolutionary tools in the microwave, IR and optical regions.[30,31] One of the major successes of femtosecond pump probe spectroscopy is the establishment of the field of femtochemistry which addresses the fundamental time scale at which molecular motion occurs.[31] Extensions of the pump-probe scheme into the X-ray region is at the cutting edge of current X-ray science.

The IR - X-ray pump-probe technique is composed by two steps as illustrated in Fig.3.1. In the first step a strong IR field excites the molecular system vibrationally and the wave packet propagation is initiated in the ground state potential. After that, at a certain delay time, a short X-ray pulse promotes the wave packet to a certain point of the core excited/ionized potential. As one can see from Fig.3.1 the change of the delay time allows to map approximately the shape of the potential of the core excited/ionized state. This gives unique opportunity to detect directly the spectral transitions in the proton transfer state which form a lower energy band (see band PT in Fig.3.1). Such a detection of the proton transfer state is almost impossible using other nowadays available X-ray spectroscopies due to the extremely short life time of the core ionized state. The ultra fast X-ray snapshots of the nuclear wave packet in the ground state potential make the X-ray pump probe spectra very sensitive to the phase of the IR pulse, and to the duration and delay time of the X-ray pulse. The coherent excitation of vibrational levels by a strong IR field is a key feature of IR - X-ray pump probe spectroscopy. This motivates us to recall the principles of IR spectroscopy.

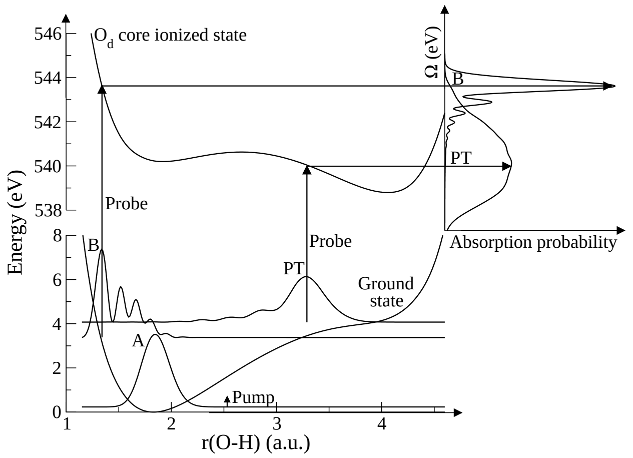

Figure 3.1: Formation of the O1s X-ray absorption spectrum of water dimer in a strong IR field.

3.1 Principle of IR spectroscopy

The frequencies of molecular vibrations span the IR region. Different functional groups of the molecule have specific vibrational frequencies which makes IR spectroscopy a powerful tool in studies of the molecular structure and molecular interaction.[32,33] To illustrate the principle of IR spectroscopy we consider a diatomic molecule with zero electronic momentum. When the IR field with the frequency ω_L exposes the molecule it excites the vibrational levels ν and rotational states $|JM\rangle$ with the probability

$$\propto \sum_{JM} \frac{|\langle J'M'|\mathbf{e}_L \cdot \mathbf{d}_{\nu 0}|JM\rangle|^2}{(\omega_L - \omega_{\nu J',0J})^2 + \gamma^2}\, \rho_J, \quad \mathbf{d}_{\nu 0} = \langle \nu|\mathbf{d}|0\rangle. \tag{3.1}$$

Here $\omega_{\nu J',0J}$ is the resonant frequency of the rotational-vibrational transition, γ is the width of the IR transition. The IR spectrum strongly depends on the temperature through the Boltzmann distribution of rotational levels, ρ_J. It is to note that the vibrational spectrum has fine structure caused by rotational transitions. We see from eq.(3.1) that vibrational transitions are allowed only when the gradient of the molecular dipole moment, $d'(r_0) =$

$\partial d(r)/\partial r|_{r=r_0}$ is different from zero

$$\langle 0|d(r)|\nu\rangle = d' \; \langle 0|x|\nu\rangle \propto \delta_{\nu,1}. \tag{3.2}$$

Here $x = r - r_0$ and r_0 is the equilibrium internuclear distance. The r-dependence of the molecular dipole moment is illustrated in Fig.3.2 for the water dimer. The excitation of rotational levels origins from the angular dependence of the scalar product of $\mathbf{d}_{\nu 0}$ and polarization vector of the IR photon, $\mathbf{e}_L$: $\mathbf{e}_L \cdot \mathbf{d}_{\nu 0} \propto \cos\theta$.

In the current thesis the rotational degrees of freedom are treated classically, which is a reasonable approximation because the rotational structure is not resolved in X-ray spectra due to the large lifetime broadening. We will also ignore the weak temperature population of the vibrational levels.

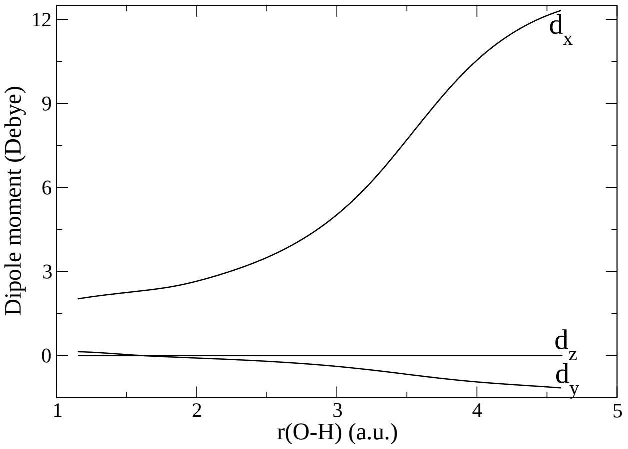

Figure 3.2: Dependence of the dipole permanent dipole moment of the water dimer on r(O-H) bond length (see Paper III).

3.2 Proton transfer in core ionized state of water dimer

Let us explore the IR - X-ray pump probe spectroscopy in more detail for the water dimer as this technique gives a unique opportunity to investigate the dynamics of proton transfer in the core ionized state. As was mentioned already the main advantage of such a technique is that a strong IR field at the certain instant can localize the nuclear wave packet directly in the proton transfer region (see Fig.3.1).

When the IR field is incoherent the only role of the IR field is to change the populations of the vibrational levels, ρ_ν. In this case the probability of core excitation is to produce an incoherent sum of the partial probabilities, $P^{(\nu)}(\omega_X)$, of core ionization from certain vibrational levels,$|\nu\rangle$

$$P(\omega_X) = \sum_{\nu} \rho_\nu P^{(\nu)}(\omega_X). \tag{3.3}$$

This probability does not depend on the phase of the IR field (see Sec.3.3.1). This scenario changes qualitatively if the IR field is coherent having a constant phase, φ_L. The coherence of the light is transferred to the molecule. Indeed the coherent IR light creates a coherent superposition of vibrational states or wave packet

$$\begin{aligned} \phi(t) &\propto |0\rangle + a(t)|1\rangle e^{-\imath(\omega_{10}t+\varphi_L)} + \cdots \\ &\propto \left[1 + a(t)\sqrt{2}(r-r_e)/a_0 e^{-\imath(\omega_{10}t+\varphi_L)} + \cdots\right] \exp\left(-\frac{(r-r_e)^2}{2a_0^2}\right) \end{aligned} \tag{3.4}$$

where r and r_e denote the internuclear distance and equilibrium distance, respectively. a_0 is the amplitude of vibrations and the coefficient $a(t)$ is proportional to the strength of electromagnetic interaction. One finds that the characteristic time of the wave packet propagation is given by the period of vibrations $2\pi/\omega_{10}$. Eq. (3.4) explains the physical ground of the wave packet propagation in the potential well. This dynamics is quenched when the phase randomly fluctuates (incoherent light). Thus the coherence of IR field is the key element of the here discussed X-ray pump-probe spectroscopy and it makes the X-ray ionization/absorption profile sensitive to the phase φ_L.

To observe the proton transfer state in the X-ray photoionization spectrum we have rather to populate the high vibrational levels, $\nu \gtrsim 9$ (see Fig.2.10). However, due to the strong anharmonicity of the ground state potential, the resonant condition breaks down and the efficiency to populate high vibrational levels by the continuum wave IR laser is strongly suppressed if the X-ray pulse is long. This difficulty is overcome for short IR pulses with rather large spectral widths, $1/\tau_L$. Our simulations (see Paper III) show that the short IR pulse with the duration $\tau_L = 7.9$ fs is able to populate vibrational states up to $\nu = 10$ for a reasonable intensity, I_L=5.4 x 10^{14} W/cm^2. This coherent IR pulse creates a nuclear wave packet (3.4) which moves in the ground state potential well along the trajectory

$$\bar{r}(t) = \langle \phi(t)|r|\phi(t)\rangle. \tag{3.5}$$

Here $\bar{r}(t)$ is the center of gravity of the wave packet. This trajectory depends strongly on the phase of the IR pulse, φ_L (Fig.3.3). This explains the strong phase sensitivity of the XPS spectrum (Fig.3.4).

The first and the second terms at the right hand-side of eq.(3.4) give an alternative and useful interpretation of the phase effect.[34] The phase dependence arises from the interference of

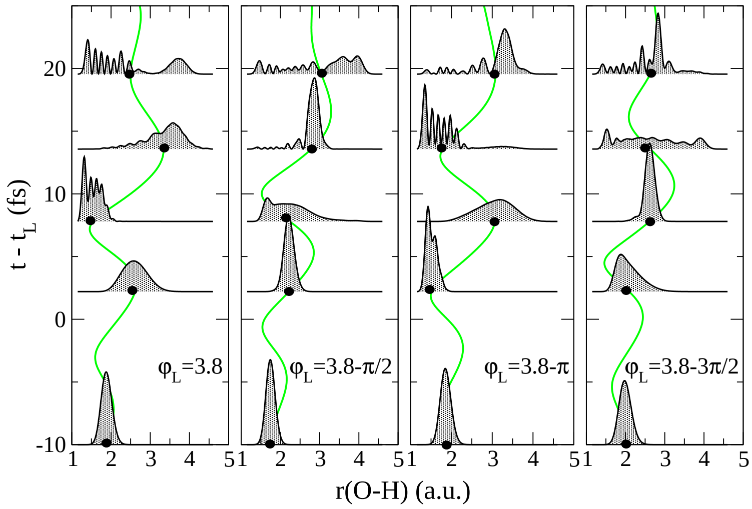

Figure 3.3: The phase dependence of the trajectory of the wave packet in the ground state potential created by a strong IR field.

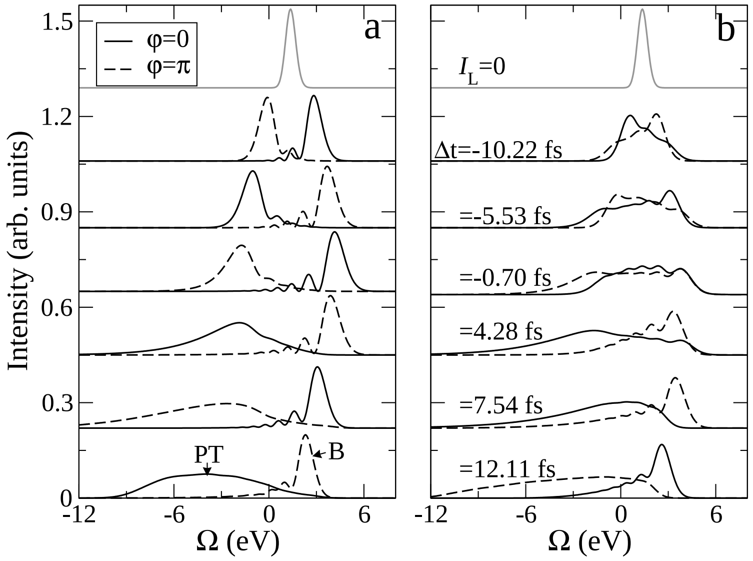

Figure 3.4: IR - XR pump-probe spectrum of the water dimer versus time delay (Δt) and different phases [(a) φ_L=3.8 rad and (b) φ_L =(3.8-π/2) rad] for different orientations (φ) of the dimer relative to the IR polarization vector. τ_L=7.9 fs, I_L=5.4 x 10^{14} W/cm^2 and $\omega_L = \omega_{01}$=0.45 eV. The duration of the X-ray pulse is τ_X = 2.2 fs.

one- and two-photon core ionization channels: direct absorption of an X-ray photon from the lowest vibrational state $\nu = 0$ and absorption of an X-ray photon from the next vibrational level $\nu = 1$ which is populated by one IR photon (see Fig.3.5). At the instant when the wave packet arrives at the proton transfer region the short X-ray pulse excites the molecular system in the proton transfer site (see Fig.3.1). The XPS band related to this transition has lower energy (see Fig.2.10) and due to this circumstance the proton transfer (PT) band is nicely distinguished in the XPS spectrum, Fig.3.4, at low energy.

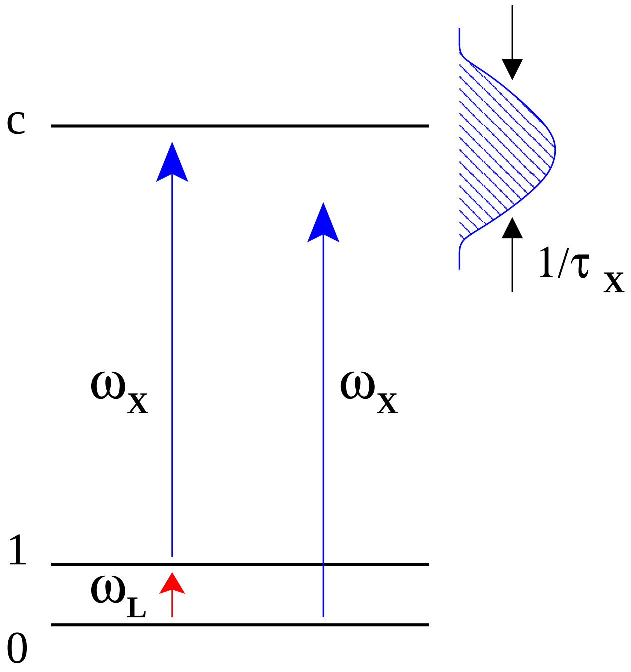

Figure 3.5: Interference of one- and two-photon channels of core electron excitation.

The profile of the X-ray pump-probe spectrum turns out to be very sensitive in several respects; it is sensitive to the phase of the IR field, to the orientation of the molecular system relative to the IR polarization vector, as well as to the delay time (Δt) and the duration time (τ_X) of the X-ray pulse. The molecules are usually randomly oriented which means that the XPS spectra (Fig.3.4) have to be averaged over molecular orientations. The X-ray pump probe spectra of randomly oriented molecules differ considerably from spectra of fixed-in-space molecules (see Paper III). It is necessary to note that powerful techniques exist in X-ray spectroscopy which allows to obtain spectra of fixed-in-space molecules even for randomly oriented samples.[10,35,36] This follows from the fact that the core excited state experiences Auger decay to a multitude of final states most of which are dissociative. The detection of the ionic fragment of dissociation thus selects a certain orientation of the molecule. The measurement of X-ray absorption in the ion yield mode or detection of photoelectron in the coincidence with the ion are widely used in studies of X-ray spectra of fixed-in-space molecules.[10,35,36] These method is thus nicely adapted for the observation of the discussed phase effect.

3.3 Role of light coherence, duration and phase

We outlined the principles of IR - X-ray pump probe spectroscopy in the previous chapter. Now we would like to highlight some important features of this spectroscopy making use of a simple system the NO molecule.

3.3.1 X-ray spectrum in the field of incoherent pump radiation

As was mentioned above even incoherent pump radiation influences the probe X-ray spectra, see eq.(3.3).

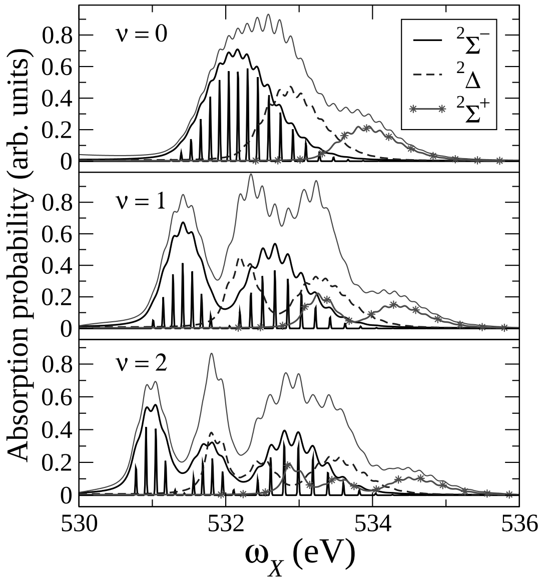

Figure 3.6: Partial OK X-ray absorption spectra of NO excited incoherently in the ground state vibrational levels $\nu = 0,\ 1,\ 2$ for different core excited electronic states: $^2\Sigma^-$, $^2\Delta$ and $^2\Sigma^+$. The total spectral profiles are shown by the thin continuum lines.

The main distinction of X-ray spectra of molecules driven by incoherent pump radiation is that such a pump field lacks a certain weak-defined phase and can therefore not create a coherent nuclear wave packet. In this case the X-ray spectrum becomes a sum of partial spectra corresponding to different vibrational levels of the ground state. The partial OK X-ray absorption spectra of the NO molecule differ strongly from each other (Fig.3.6), which can be referred to the different Franck-Condon distributions for different initial vibrational states ν (see Paper IV).

3.3.2 Role of duration of X-ray and IR pulses

Let us now explore the X-ray spectra of molecules in the strong field of coherent IR radiation. To be specific only the lowest OK X-ray $^2\Pi \rightarrow ^2\Sigma^-$ absorption band will be considered.

The duration (τ_X) of the X-ray pulse ($E_X(t) = E_X^0 \exp[-((t-t_X)/\tau_X)^2 \ln 2/2]$) influences strongly the phase effect (Fig.3.7). The role of the duration of the X-ray pulse is seen from eq.(3.4). This equation indicates that the interference contribution in the X-ray excitation probability experiences oscillations with the vibrational frequency

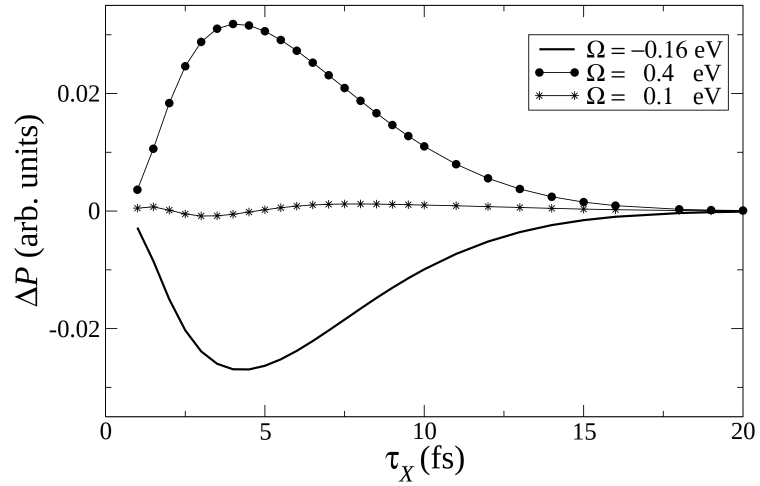

Figure 3.7: Difference between probabilities of X-ray absorption (O1s → 2π) of NO, $\Delta P = P(\varphi_L = 0) - P(\varphi_L = \pi/2)$ versus duration of X-ray pulse, τ_X. Δt=610 fs.

$$P_{\rm int}(t) \propto \Re e \; E_X(t) \; e^{\imath(\omega_{10} t + \varphi_L)}. \qquad (3.6)$$

When the pulse is long: $\tau_X \gg 2\pi/\omega_{10}$, the integration of $P_{\rm int}(t)$ over the time of measurement quenches the interference term. So the phase sensitivity of the X-ray spectrum is suppressed for long X-ray pulses. The phase effect takes maximum value when τ_X is one fourth of the period of vibrations, $\pi/2\omega_{10}$ (see Fig.3.7). In the opposite limiting case, $\tau_X \ll 2\pi/\omega_{10}$, the interference and, hence, the phase effect is also suppressed. The reason for this is that short X-ray pulses have broad spectra. The convolution of the X-ray spectra depicted in Fig.3.4 with such a broad spectrum strongly diminishes the phase sensitivity of the X-ray profile.

The duration of the IR pulse affects the X-ray profile in another way. As it was mentioned above the shortening of the IR pulse can be useful to overcome the anharmonicity which prevents the excitation of high vibrational levels. The temporal shape of the IR pulse influences strongly the memory effect discussed in the next section.

3.3.3 Phase memory versus shape of the IR pulse

The vibrational levels of the ground electronic state of a gas phase molecule have rather long lifetimes; $\lesssim 1$ ms for diatomic molecules. This means that the coherence created by the IR pulse lives a long time after that the IR pulse left the system. This also means that the X-ray spectra continue to be sensitive to the phase during a long time. Such a memory effect depends strongly on the shape of the IR pulse (see Paper IV). The memory effect is destroyed if the IR pulse is switched off adiabatically. This physical picture of the memory effect is illustrated in Fig.3.8. We see that the population of the first vibrational state follows the Rabi solution[37]

$$\rho_1(t) \approx \sin^2 \frac{G_R t}{2}, \quad G_R = \mathbf{E}_L \cdot \mathbf{d}_{10}. \tag{3.7}$$

Fig.3.8A shows the case of fast off-switching of the IR field: The duration of the IR pulse is then shorter than the Rabi period, $T_R = 2\pi/G_R$. In this case the molecule remains in the coherent superposition of vibrational states and the X-ray spectrum keeps the phase memory after that the IR pulse left the system.

The opposite case of adiabatic shut down of the IR radiation ($\Delta T \gtrsim T_R$) is shown in Fig.3.8B. In this case the molecule follows adiabatically the slow decrease of the IR intensity and the molecule evolves to the lowest vibrational state. In this case the molecule looses memory about the phase and the X-ray spectrum ceases to depend on the phase after that the IR pulse left the system (see Paper IV).

3.3.4 Dephasing caused by z-dependence of the phase of the IR field

Until now we assumed that the phase of the IR field is constant. This is not true in general due to phase, $k_L z$, which describes the propagation of the IR field:[34] $E_L(t)\cos(\omega_L t - k_L z +$

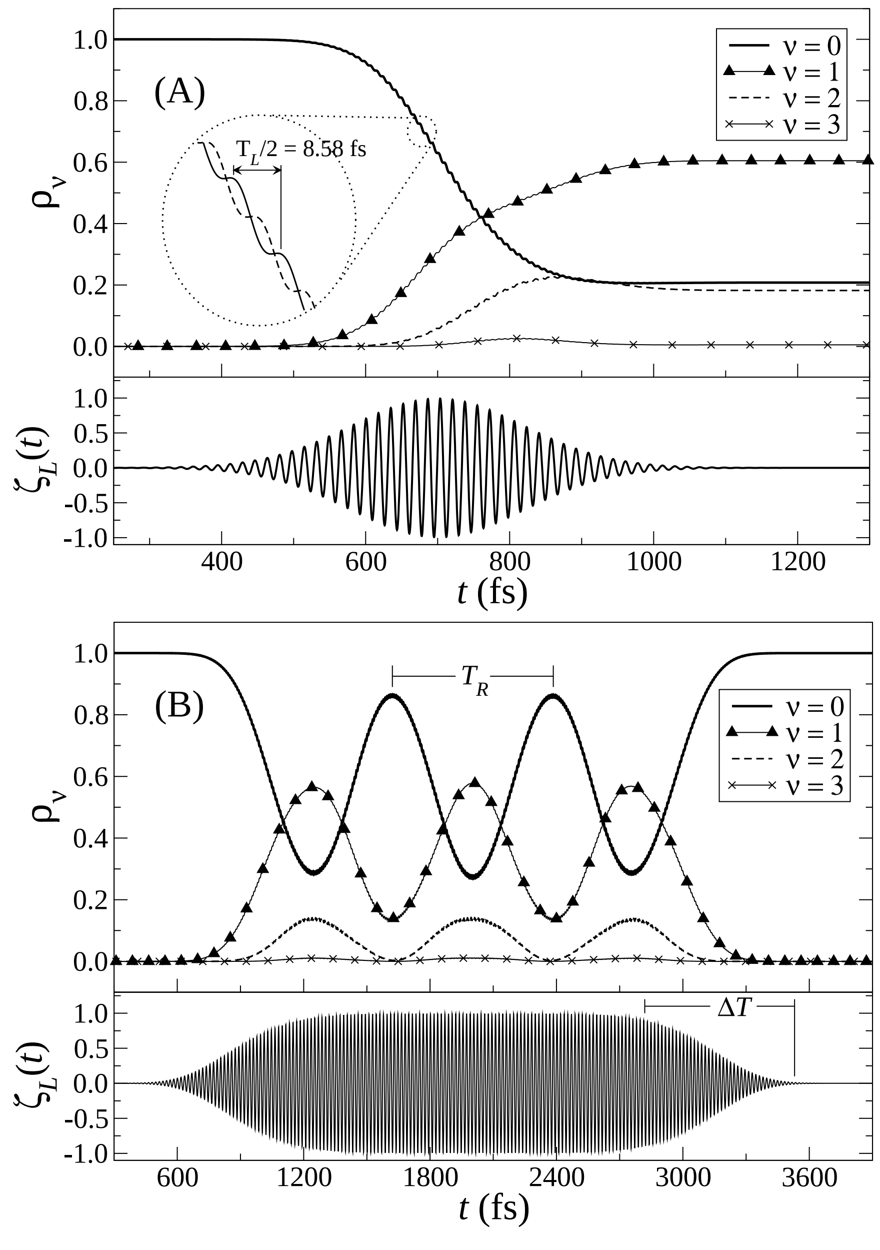

Figure 3.8: Populations (ρ_ν) of the vibrational levels of the ground state versus time for different durations of switching off of the pump field, which is $\tau_L = 100$ fs $< \mathrm{T}_R$ for short pulse (A), and $\Delta T \approx 715$ fs $\gtrsim \mathrm{T}_R$ for long pulse (B). $\zeta_L(t)$ is the shape of the envelope of IR field. The details of calculations are described in Paper IV.

φ_L). To take this extra phase into account we have to use a z-dependent phase $\varphi_L(z)$:

$$\varphi_L(z) = \varphi_L - k_L z, \quad k_L = \frac{2\pi}{\lambda_L} \tag{3.8}$$

where $\varphi_L = \text{const}$. If the size of the irradiated region is larger than the wave length of the IR field, λ_L, the z-dependence of the phase (3.8) can quench the phase effect, because the X-ray spectrometer collects signals from molecules localized in different points, z. To avoid this difficulty one can use the orthogonal intersection of the X-ray and IR beams (Fig.3.9) with the size of X-ray beam

$$a \lesssim \lambda_L \sim 10^{-3} \text{ cm}. \tag{3.9}$$

The focusing of the X-ray beam in such a spot is possible in current experiments.[38]

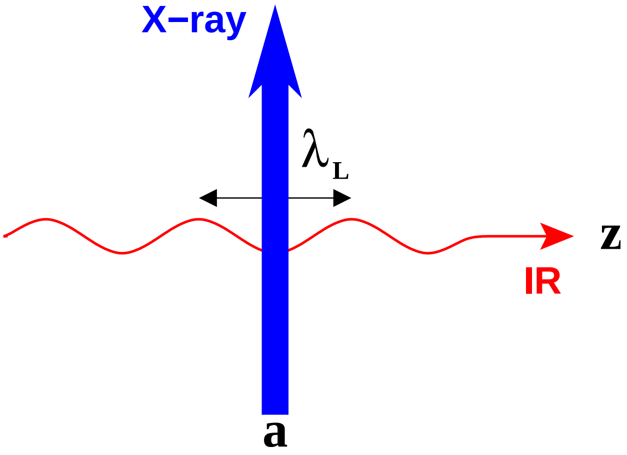

Figure 3.9: Orthogonal orientation of X-ray and IR beams which allows to reduce the dephasing caused by the phase factor, $k_L z$.

Chapter 4

Conclusion

• It is shown that NEXAFS spectroscopy can evidence through-space and through-bond interactions of unoccupied orbitals.

• Core ionization of the donor oxygen of the water dimer results in a drastic change of the potential, exhibiting the global minimum in the proton transfer region.

• The O1s photoelectron spectrum of the water dimer shows a significant qualitative difference from the monomer spectrum. The weak hydrogen bonding and the big change of the water dimer potential under core ionization are responsible for the anomalously strong vibrational broadening: 0.4 eV for the acceptor band and 0.6 eV for the donor band.

• It is shown that X-ray pump probe spectroscopy is a proper tool to explore the proton transfer in the water dimer under core ionization contrary to conventional XPS spectroscopy.

• It is shown that the trajectory of the nuclear wave packet changes drastically under change of the phase of the driving IR field.

• A new type of spectroscopy is proposed - phase sensitive IR - X-ray pump probe spectroscopy.

• A dynamical theory of phase sensitive IR - X-ray pump probe spectroscopy is developed.

• The phase sensitivity of X-ray spectra of molecules driven by a strong IR field depends strongly on the duration of the X-ray pulse, the delay time, the shape of the IR pulse and on the orientational ordering of the sample.

Bibliography

[1] R. Hoffmann. *Acc. Chem. Res.*, 4:1, 1971.

[2] R. Hoffmann, A. Imamura, and W. J. Hehre. *J. Am. Chem. Soc.*, 90:1499, 1968.

[3] M. Drescher, M. Hentschel, R. Klenberger, M. Ulberacker, V. Yakovlev, A. Scrinzl, T. H. Westerwalbesloh, U. Kleineberg, U. Heinzmann, and F. Krausz. *Nature*, 419:803, 2002.

[4] R. W. Schoenlein, S. Chattopadhyay, H. H. W. Chong, T. E. Glover, P.A. Heimann, W. P. Leemans, C. V. Shank, A. Zholents, and M. Zolotorev. *Appl. Phys. B*, 71:1, 2000.

[5] R. W. Schoenlein, W. P. Leemans, A. H. Chin, P. Volfbeyn, T. E. Glover, P. Balling, M. Zolotorev, K. J. Kim, S. Chattopadhyay, and C. V. Shank. *Science*, 274:236, 1996.

[6] A. Zholents and W. M. Fawley. *Phys. Rev. Lett.*, 92:224801, 2004.

[7] B. W. Adams. *Rev. Sci. Instrum.*, 75:1982, 2004.

[8] J. Stöhr. *NEXAFS Spectroscopy.* Springer, Berlin, 1992.

[9] S. Svanberg. *Atomic and Molecular Spectroscopy.* Springer-Verlag, Berlin, Heidelberg, New York, 2001.

[10] K. Ueda. *J. Phys. B: At. Mol. Opt. Phys.*, 36:R1, 2003.

[11] F. Gel'muchanov and H. Ågren. *Phys. Rep.*, 312:87, 1999.

[12] J. E. Rubensson. *J. Electron Spectrosc. Rel. Phen.*, 110-111:135, 2000.

[13] J. Guo and J. Nordgren. *J. Electron Spectrosc. Rel. Phen.*, 110-111:105, 2000.

[14] M. N. Piancastelli. *J. Electron Spectrosc. Rel. Phen.*, 107:1, 2000.

[15] S. L. Sorensen and S. Svensson. *J. Electron Spectrosc. Rel. Phen.*, 114-116:1, 2001.

[16] P. A. Brühwiler, O. Karis, and N. Mårtensson. *Rev. Mod. Phys.*, 74:703, 2002.

[17] E. Kukk. *J. Electron Spectrosc. Rel. Phen.*, 127:43, 2002.

[18] G. B. Armen, H. Åberg, and S. Aksela. *J. Phys. B: At. Mol. Opt. Phys.*, 33:49, 2000.

[19] K. Siegbahn, C. Nordling, G. Johansson, J. Hedman, P. F. Hedén, K. Hamrin, U. Gelius, T. Bergmark, L. O. Werme, R. Manne, and Y. Baer. *ESCA Applied to Free Molecules.* North-Holland, Amsterdam, 1969.

[20] L.N. Mazalov, F.Kh. Gel'mukhanov, and V.M. Chermoshentsev, *Zh.Strukt.Khim.*, 15:1099, 1974. [*J.Struct.Chem.*, 15:975, 1974].

[21] J.L. Dehmer and D. Dill, *Phys. Rev. Lett.*, 35:213, 1975.

[22] V.I. Nefedov, *Zh.Strukt.Khim.*, 11:292, 1970. [*J.Struct.Chem.*, 11:272, 1970].

[23] H. Köppel, W. Domcke, and L. S. Cederbaum. *Adv. Chem. Phys.*, 57:59, 1984.

[24] H. Ågren, A. Cesar, and C. M. Liegener. *Adv. Quant. Chem.*, 23:1, 1992.

[25] F. Gel'mukhanov and H. Ågren. *J. Phys. B: At. Mol. Opt. Phys.*, 28:3699, 1995.

[26] A. Modelli and P. D. Burrow. *J. Phys. Chem.*, 88:3550, 1984.

[27] J. T. Francis and A. P. Hitchcock. *J. Phys. Chem.*, 96:6598, 1992.

[28] U. Buck and F. Huisken. *Chem. Rev.*, 100:3863, 2000.

[29] R. Sankari, M. Ehara, H. Nakatsuji, Y. Senba, K. Hosokawa, H. Yoshida, A. De Fanis, Y. Tamenori, S. Aksela, and K. Ueda. *Chem. Phys. Lett.*, 380:647, 2003.

[30] W. Demtroder. *Laser Spectroscopy.* Springer-Verlag, Berlin, 3rd edition, 1996.

[31] A. H. Zewail. *Femtochemistry: Ultrafast Dynamics of the Chemical Bond*, volume I, II. World Scientific Publishing Co. Pte. Ltd., Singapore, 1994.

[32] G. Herzberg. *Molecular Spectra and Molecular Structure I, Spectra of Diatomic Molecules.* Van Nostrand, Princeton, N.J., 2nd edition, 1950.

[33] G. Herzberg. *Molecular Spectra and Molecular Structure II, Infrared and Raman Spectra of Polyatomic Molecules.* Van Nostrand, Princeton, N.J., 1945.

[34] F. F. Guimarães, V. Kimberg, F. Gel'mukhanov, and H. Ågren. *Phys. Rev. A*, 2004. accepted.

[35] A. Yagishita, E. Shigemasa, and N. Kosugi. *Phys. Rev. Lett.*, 72:3961, 1994.

[36] R. Guillemin, E. Shigemasa, K. Le Guen, D. Ceolin, C. Miron, N. Leqlercl, K. Ueda, P. Morin, and M. Simon. *Rev Sci. Instrum.*, 71:4387, 2000.

[37] M. O. Scully and M. S. Zubairy. *Quantum Optics.* Cambridge University Press, Cambridge, 1997.

[38] J. Wang, A. K. Sood, P. V. Satyam, Y. Feng, X-Z. Wu, Z. Cai, W. Yun, and S. K. Sinha. *Phys. Rev. Lett.*, 80:1110, 1998.